Distributions of glass-transition temperature and thermal expansivity in multilayered polystyrene thin films studied by neutron reflectivity

Rintaro Inoue,[1] Kazuko Kawashima,[1] Kazuya Matsui,[1] Toshiji Kanaya,[1,*] Koji Nishida,[1] Go Matsuba,[2] and Masahiro Hino[3]

[1]*Institute for Chemical Research, Kyoto University, Uji, Kyoto-fu 611-0011, Japan*

[2]*Faculty of Science and Engineering, Yamagata University, 4-3-16 Jonan, Yonezawa, Yamagata 992-8510, Japan*

[3]*Research Reactor Institute, Kyoto University, Kumatori-cho, Sennan-gun, Osaka-fu 590-0494, Japan*

(Received 18 July 2010; published 8 February 2011)

We performed neutron reflectivity measurements on multilayered polymer thin films consisting of alternatively stacked deuterated polystyrene (*d*-PS) and hydrogenated polystyrene (*h*-PS) layers ∼200 Å thick as a function of temperature covering the glass-transition temperature T_g, and we found a wide distribution of T_g as well as a distribution of the thermal expansivity α within the thin films, implying the dynamic heterogeneity of the thin films along the depth direction. The reported anomalous film thickness dependences of T_g and α were reasonably understood in terms of the distributions, showing that the surface mobile layer and the bottom hard interfacial layer are, respectively, responsible for the depressions of T_g and α with decreasing film thickness. The molecular mobility in each layer is also discussed in relation to the distribution of T_g, based on the results on mutual diffusion at the layer interface.

DOI: 10.1103/PhysRevE.83.021801 PACS number(s): 61.41.+e, 64.70.pj, 68.60.Dv, 61.05.fj

I. INTRODUCTION

It was reported that thermal and mechanical properties of polymer thin films were quite different from those of bulk state [1,2]. One of the most fascinating topics is the thickness dependence of glass-transition temperature T_g, which has been studied extensively by various methods [3–9], including ellipsometry [3,4], x-ray and neutron reflectivity [5,6], positron annihilation lifetime spectroscopy (PALS) [7], dielectric relaxation [8], and inelastic neutron scattering [9]. For polystyrene (PS) thin films supported on silicone (Si) substrate, the reduction of T_g was observed with decreasing film thickness [4]. The result is often interpreted in terms of a surface mobile layer, implying the heterogeneous dynamics of polymer thin films along the depth direction. Some works have directly revealed the surface mobile layer [10,11]. Another interesting finding is the depression of thermal expansivity α with decreasing film thickness [5–7]. In a previous paper [12], we showed that the molecular mobility in PS thin films decreased with the film thickness due to the hard layer near the substrate, which must be a possible reason for the depression of α with the film thickness. This result also supports the heterogeneity of polymer thin films along the depth direction.

It is essential to reveal the dynamic heterogeneity to understand the anomalous nature of polymer thin films as de Gennes pointed out [13]. Therefore, in this paper we study the distributions of T_g and the thermal expansivity α in PS thin films. We performed neutron reflectivity measurements on multilayered PS thin films consisting of alternatively stacked deuterated and hydrogenated polystyrene (*d*-PS and *h*-PS) layers. We also discuss the interdiffusion of *d*-PS and *h*-PS layers to reveal the correlation between T_g and the molecular mobility.

II. EXPERIMENTAL

We used *h*-PS with a molecular weight M_w of 7.69×10^5 and molecular weight distributions M_w/M_n of 1.18, and *d*-PS with a molecular weight M_w of 7.31×10^5 and molecular weight distributions M_w/M_n of 1.08. The bulk T_g's determined by differential scanning calorimetry (DSC) were 376 ± 2 K for both *h*-PS and *d*-PS. We prepared *d*-PS/*h*-PS/*d*-PS three-layer and *d*-PS/*h*-PS/*d*-PS/*h*-PS/*d*-PS five-layer thin films with a component layer ∼200 Å. The following procedures were used for the preparation of multilayered thin films. First we prepared a *d*-PS layer directly onto a 3-in.-diam Si substrate by spin-coating toluene solutions at 2000 rpm and dried in a vacuum oven at 343 K for 24 h after drying in a vacuum oven at room temperature for 2 days to remove a residual solvent. The residual solvent in polymer thin films is a matter of discussion and some researchers studied this problem using chromatography, neutron reflectivity, and Fourier transform infrared spectroscopy [14–16]. Recently, Zhang *et al.* studied the residual solvent in PS and polymethyl methacrylate (PMMA) thin films [16] and found that no trace of solvent was observed even for as-deposited PS thin films, indicating that our drying condition was enough to remove the residual solvent in thin films. For the preparation of the subsequent layers in multilayered thin films, we used the water-floating method [17,18]. We immersed a 4-in.-diam Si substrate into 80:20 volume ratio solutions of concentrated H_2SO_4 (97%) and H_2O_2 (34.5%) at 393 K for 30 min and rinsed with water and ethanol several times to remove a residual H_2SO_4-H_2O_2 solution. After the surface treatment with H_2SO_4-H_2O_2 solution, we prepared an *h*-PS layer onto a 4-in.-diam Si substrate with a hydrophilic surface by spin-coating toluene solutions at 2000 rpm. Such a prepared thin film (*h*-PS layer) was transferred from the 4-in. Si substrate onto a water surface and collected onto the first *d*-PS layer, which was already prepared on a 3-in.-diam Si substrate. The collected *h*-PS/*d*-PS bilayer thin film was then dried in the vacuum oven with the same drying process as described above. In addition to the problems of residual solvent in the thin

*Author to whom all correspondence should be addressed: kanaya@scl.kyoto-u.ac.jp.

films, we also have to be concerned with the water immersion to the polymer thin films due to the water-floating method. Seo *et al.* studied the interfacial structure at the interface between *d*-PS and D_2O by neutron reflectivity and found that no significant structure formation caused by water inclusion to the thin film was observed [19]. Considering the reported results by Zhang *et al.* and Seo *et al.*, our drying condition of thin films was appropriate for the removal of residual solvent or water. Prior to the preparation of the subsequent layers in multilayered thin films, we checked the homogeneity of the surface structure of films by atomic force microscopy (AFM) and a confocal microscope. Repeating the same procedures, we could finally obtain *d*-PS/*h*-PS/*d*-PS three-layer or *d*-PS/*h*-PS/*d*-PS/*h*-PS/*d*-PS five-layer thin films. In our former publication [20], we studied the distribution of T_g using the five-layer thin film annealed at 363 K for 12 h, which was about 10 K below bulk T_g. Under such an annealing condition, we could not evaluate the distribution of T_g in thin films directly because all of the component layers exhibited negative thermal expansivities. We just discussed the pseudodistribution of T_g in the thin film, focusing on the temperature dependence of the film thickness of component layers only. From the former works, we recognized that annealing thin films at above bulk T_g was indispensable for a reliable evaluation of the distribution of T_g and α in thin films [5]. On the other hand, annealing for too long above T_g causes the *h*-PS layers and *d*-PS layers to mix up due to interdiffusion, and an evaluation of T_g at different layers would be impossible as a result. Considering the balance between the structural relaxation and the mutual interdiffusion, we annealed the thin films at 403 K for 5 min. The details of the annealing effect on the multilayered thin films will be reported elsewhere. The neutron reflectivity measurements were done with a MINE-II reflectometer [21] installed at the JRR-3 reactor, Tokai, and the measurements were performed at temperatures from 298 to 403 in a vacuum cell. To avoid the interdiffusion between different layers, especially above bulk T_g, the data acquisition time at each temperature was limited to 1.5 h.

III. RESULTS AND DISCUSSION

The angler dependence of the neutron count was obtained as raw data and the neutron count was converted to the reflectivity by dividing by the count of the direct beam with the same configuration. After converting the measured angles to a Q value, we got the Q dependence of reflectivity. Figure 1 shows the observed neutron reflectivity (NR) profiles from *d*-PS/*h*-PS/*d*-PS three-layer thin films at several temperatures below and above bulk T_g. For our data analysis, we used a program that was based on a recursion formula derived by Parratt [22]. Wallace *et al.* reported that the density of PS thin films was the same as that of bulk within 0.5% experimental error by NR [23], hence we decided to use the bulk scattering length density (SLD) for *d*-PS and *h*-PS to our fits. Using the bulk SLD values of *h*-PS and *d*-PS for the *h*-PS and *d*-PS layers, respectively, we evaluated the thickness and the interfacial roughness described by an error function. The three-layer model could describe the experimental results from the three-layer thin film well. The evaluated temperature dependence of the total film thickness is shown in the top part of Fig. 2. The change of the thermal

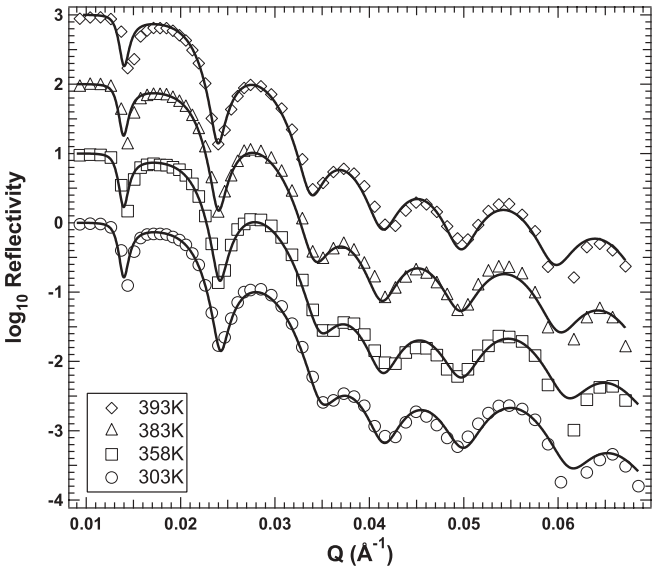

FIG. 1. Neutron reflectivity profiles from three-layer thin film at 303, 358, 383, and 393 K (solid lines) are the results of fit using a three-layer model. For clarity, each reflectivity profile is shifted vertically.

expansivity between the glassy state and the molten state was used to determine T_g. The evaluated T_g of the total thickness is 374 K, which is almost the same as the bulk T_g (=376 K). Thermal expansivities in the glassy and molten states were 9.4×10^{-5} and 4.9×10^{-4} K^{-1}, respectively, and these values are almost the same as the bulk values (1.1×10^{-4} and 5.1×10^{-4} K^{-1}) [5]. The total thickness of the three-layer film, ~640 Å thick, was similar to that of a bulk sample.

We evaluated the temperature dependence of the film thickness of each layer, which were termed the first, second, and third layer from the bottom to the top, as shown in Fig. 2. Each layer showed a very different temperature dependence of the thickness. The third and second layers showed clear changes of the thermal expansivity at T_g's. Miyazaki *et al.* [24] reported that annealing at above bulk T_g for a short time was enough for the reliable determination of T_g and thermal expansivity, and the values of T_g and thermal expansivity were not affected by annealing time. Our annealing condition was enough for the evaluation of the distribution of T_g and thermal expansivity in multilayered thin films. The T_g's shown by solid arrows in Fig. 2 were evaluated from the linear least-squares fit to the data in both glassy and molten states, and the evaluated T_g's for the third and second layers are 358 and 374 K, respectively. The T_g of the third layer is much lower than the bulk T_g (=376 K), while the latter is close to the bulk T_g. We also estimated the minimum T_g (min T_g) and the maximum T_g (max T_g) for the evaluation of errors of T_g, considering the errors of the slopes and the intercepts, which were estimated from the linear least-squares fits. The min T_g and max T_g were also shown by dashed arrows and dotted arrows, respectively, in Fig. 2. From the values of min T_g and max T_g, we found that the errors in the evaluated T_g were at most ± 5 K.

Surprisingly, the film thickness of the first layer is almost independent of temperature, corresponding to zero thermal

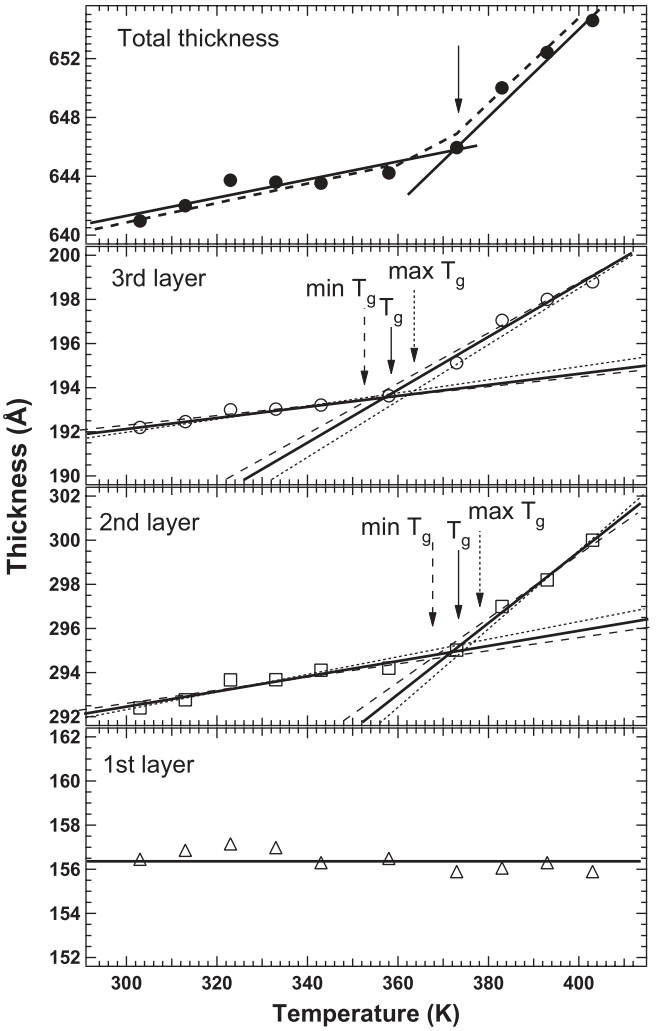

FIG. 2. Temperature dependence of total film thickness, first layer, second layer, and third layer from bottom to top, for the three-layer thin film (solid arrows) corresponding to the evaluated T_g of each layer. Dashed and dotted arrows in the box of the second layer and the third layer correspond to the estimated minimum T_g (min T_g) and maximum T_g (max T_g). Dotted line in the top figure indicates the temperature dependence of the total film thickness calculated from the thickness of the component layer at room temperature and the distribution of thermal expansivities.

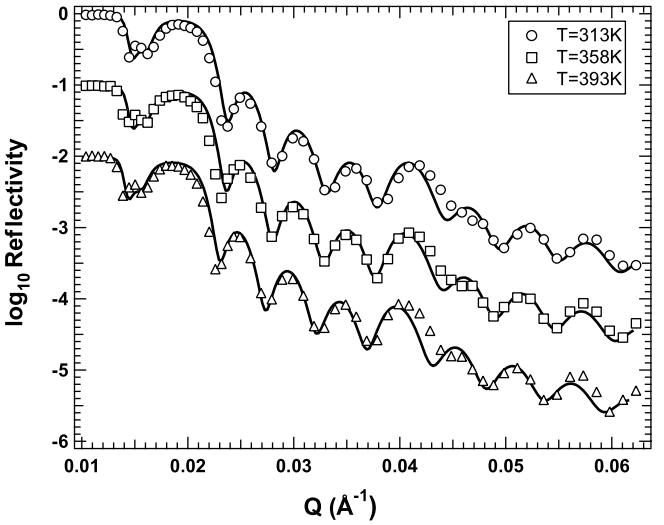

FIG. 3. Neutron reflectivity profiles from the five-layer thin film at 313, 358, and 393 K (solid lines) are the results of fit using a five-layer model. For clarity, each reflectivity profile is shifted vertically.

expansivity, and it does not show any upturn in the temperature range examined, suggesting that the T_g of the first layer was so high as to be out of the temperature range of the measurement. NR measurements were also performed on the five-layer thin film, and the five-layer model could describe the results well at below and above bulk T_g, as shown in Fig. 3. The temperature dependence of the total film thickness given in the top of Fig. 4 (∼1000 Å) showed bulk T_g and bulk thermal expansivity, implying that the total film thickness also exhibited bulk behavior for the five-layer thin film. We termed each component layer the first, second, third, fourth, and fifth layer from the substrate to the interface between the polymer and air, and the temperature dependence of each component layer is given in Fig. 4. In principle, we observed similar results to those of the three-layer film: The fifth layer shows lower T_g than the bulk T_g, and the first layer shows almost zero thermal expansivity, suggesting a higher T_g than the temperature range examined. For the five-layer thin film, we also estimated ±5 K errors for the evaluated T_g's, following similar procedures to those used for the three-layer thin film. The evaluated T_g's are plotted as a function of average distance from the substrate in Figs. 5(a) and 5(b) for the three- and five-layer thin films, respectively.

The T_g's of the top layer (the first layer) at ∼200 Å thick are 358 and 356 K for the three- and five-layer thin films, respectively, being about 20 K below the bulk T_g. The reduction of T_g for the top layer at ∼200 Å thick is consistent with the previous works [11]. On the other hand, the bottom layers at ∼150 Å thick (the first layers for the three- and five-layer films) show the strange behavior of the zero thermal expansivity. Tanaka *et al.* observed an ∼20 K increase of T_g compared to bulk T_g at a distance about 200 Å away from the substrate for PS thin films onto SiO_x substrate [25]. The thickness of our bottom layer was ∼150 Å below 200 Å, hence more than a 20 K increase of T_g would be expected. The zero thermal expansivity of the bottom layer also supports the higher T_g than the temperature range examined. It is expected that the T_g of the bottom layer might shift to be out of the experimental temperature range (above 403 K), therefore we included a lower limit of the T_g for the bottom layer in Fig. 5. We considered a possible reason for the increase of T_g of the bottom layer. Gautam *et al.* investigated the molecular structure of PS at the interface between substrate and polymer by IR-visible sum-frequency (SFG) spectroscopy [26], and they observed a preferred perpendicular orientation of the phenyl group with respect to the surface normal, implying an in-plane orientation of the main chain at the interface. Furthermore, they also reported that the in-plane orientation structure was well kept even at 473 K, which was about 100 K above the bulk T_g, hence an in-plane orientation of polymer chains at the interface is supposed to be the main reason for the

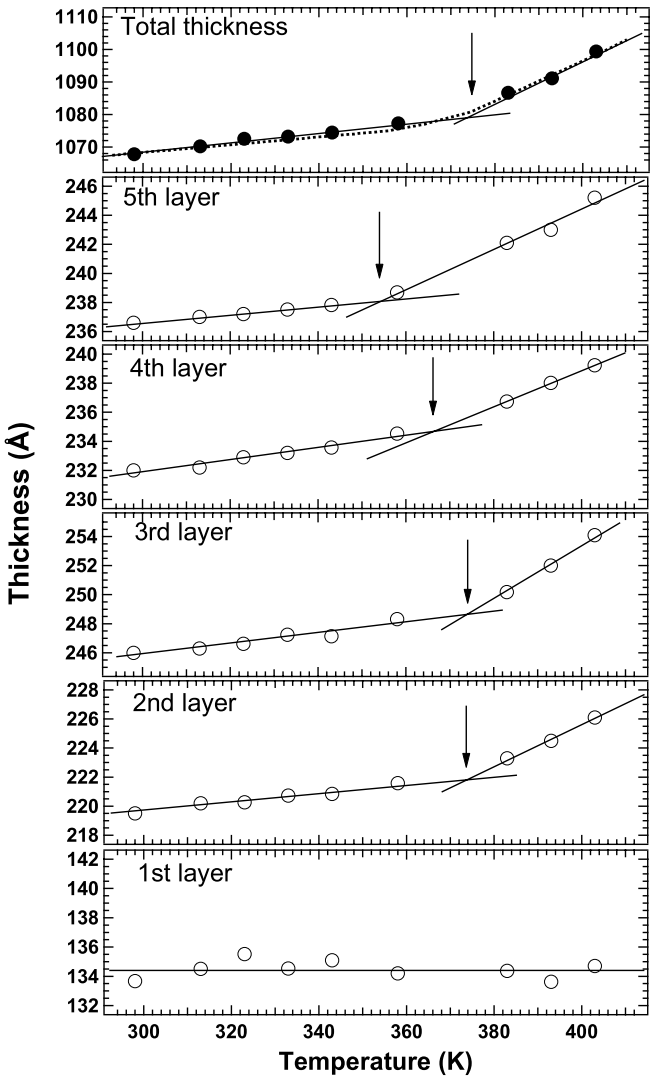

FIG. 4. Temperature dependence of total film thickness, first layer, second layer, third layer, fourth layer, and fifth layer from bottom to top, for the five-layer thin film (solid arrows) corresponding to the evaluated T_g of each layer. Dotted line in the top figure indicates the temperature dependence of the total film thickness calculated from the thickness of the component layer and the distribution of thermal expansivities.

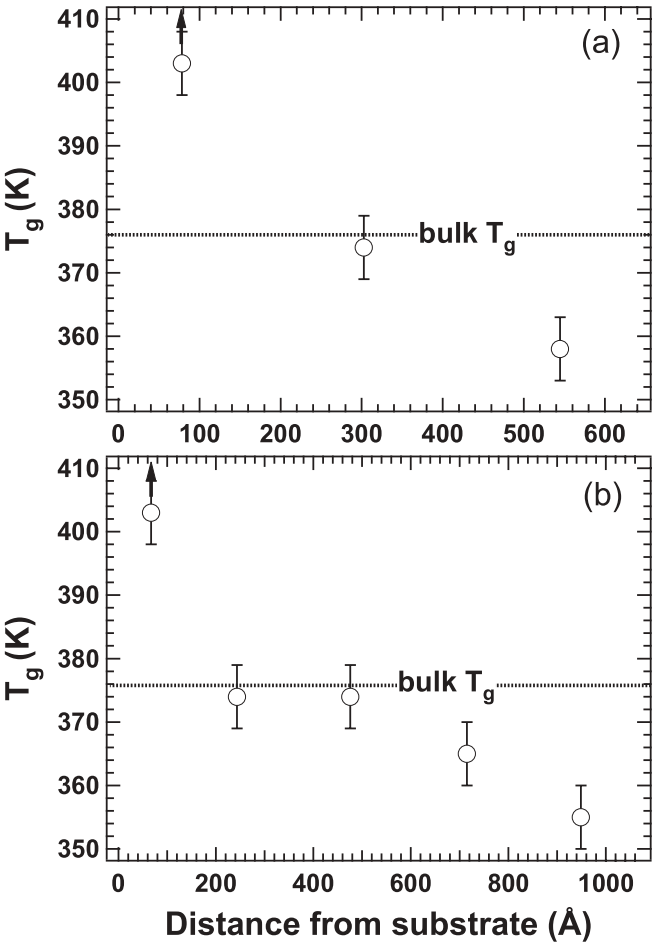

FIG. 5. Distribution of T_g of each layer for (a) the three-layer and (b) the five-layer thin film as a function of depth from the substrate; solid arrows indicates the lower limit of T_g for the interfacial layer.

dramatic increase of T_g at the interface between the polymer and the substrate.

In the three-layer thin film, the T_g of the second layer, which is located at ∼200 Å from the top layer and ∼150 Å from the substrate, is very close to the bulk T_g. Does this mean that the effects of the surface and/or the substrate do not reach the second layer? Torkelson *et al.* have shown that the effects of the surface and the substrate lasted up to ∼400 and ∼600 Å, respectively [11]. These observations suggest that the T_g of the second layer is dominated by the competition between the surface and the substrate effects. In fact, the T_g of the second layer in the five-layer thin film, which is located ∼200 Å from the surface and ∼600 Å from the substrate, is ∼364 K. It is lower than the bulk T_g by ∼12 K. This clearly shows that the effect of the surface can still reduce the T_g of the second layer, but the substrate is too far to make T_g increase, resulting in the reduction of T_g of the fourth layer in the five-layer thin film.

We discuss the reported film thickness dependence of T_g of PS thin films on the basis of the distribution of T_g. Miyazaki *et al.* studied the thickness dependence of T_g by x-ray reflectivity (XR) [5] and found that T_g was constant below about 100-Å thickness within experimental error. They discussed that the constant value of T_g below a certain film thickness was attributed to the direct detection of surface T_g (=354.5 K), and their evaluated thickness dependence of T_g was well described by a two-layer model consisting of surface T_g and bulk T_g. Our evaluated T_g's of the third and fifth layers from the three- and five-layer thin films were 358 and 356 K, respectively, and these values were quite near to the surface T_g from Miyazaki *et al.* [5], supporting the reliability of our methods. In addition to the surface mobile layer and the middle bulklike layers, we also found the interfacial (bottom) layer with the high T_g in this study, and hence we have to include the contribution of the interfacial effect. As noted above, the observed interfacial T_g in the experiment was too high to be detected in the present temperature range. As a result, an average of the surface T_g and the middle bulklike T_g's except for the interfacial T_g could be detected within the experimental temperature range, and the interfacial contribution would be

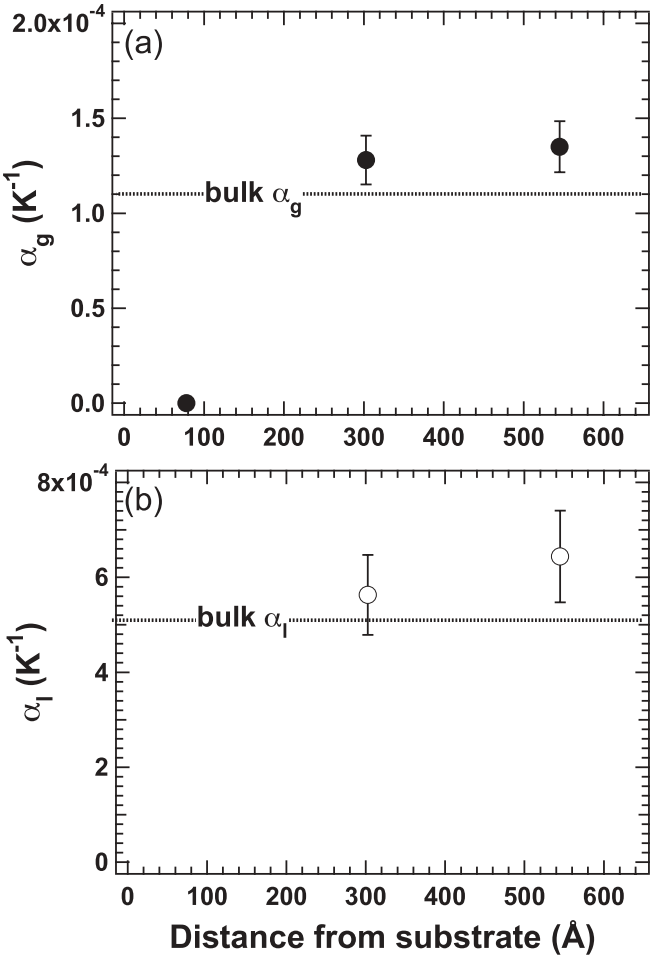

FIG. 6. Distribution of thermal expansivity in (a) a glassy state α_g and (b) a molten state α_l for the three-layer thin film as a function of depth from the substrate.

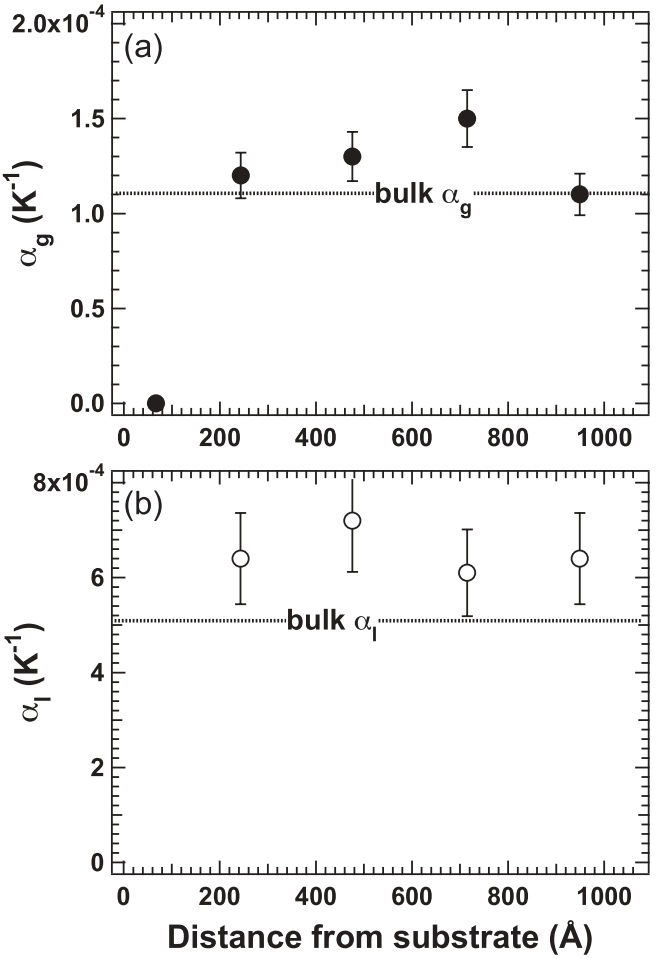

FIG. 7. Distribution of thermal expansivity in (a) a glassy state α_g and (b) a molten state α_l for the five-layer thin film as a function of depth from the substrate.

neglected. It is supposed that this is a main reason why the two-layer model worked well for the thickness dependence of T_g for the PS thin films reported so far despite the existence of the interfacial layer.

One of the advantages in the NR measurements on the multilayered films is being able to evaluate the thermal expansivity of each layer directly. We also plotted the evaluated thermal expansivity in the glassy state (α_g) and in the molten state (α_l) as a function of average distance from the substrate in Figs. 6 and 7 for the three- and five-layer thin film, respectively.

As seen in the figures, the thermal expansivities of the bottom layer (the first layers in the three- and five-layer films, respectively) are almost zero while those of the other layers are slightly larger than the bulk value [5] and independent of the location in the films. The α_g and α_l from the total film thickness are almost the same as the bulk value, which must be reproduced even including the bottom layer with the zero thermal expansivity. The thermal expansivity of the total thickness would be calculated from the average of each layer, which is given by

$$\alpha_g = \frac{1}{D}\sum_i \alpha_{g,i} d_i, \quad \alpha_l = \frac{1}{D}\sum_i \alpha_{l,i} d_i, \quad D = \sum_i d_i,$$

where D and d_i are the total film thickness and the film thickness of each layer, and $\alpha_{g,i}$ and $\alpha_{l,i}$ are the thermal expansivity of the i-th layer in the glassy state and the molten state, respectively. Using the observed distribution of α_g, α_l, we calculated the α_g, α_l of the total thickness, and found that it agreed with the observed α_g, α_l at least within the 10% experimental error. Furthermore, we also calculated the temperature dependence of the total film thickness utilizing the thickness of the component layer at room temperature and the distributions of α_g and α_l values. The results of the calculation are shown as dotted lines in the top sections of Figs. 2 and 4 for the three- and five-layer thin film, respectively, and the calculated curves could reproduce our experimental results within 10% experimental error, implying the validity of our data evaluation. DeMaggio *et al.* [7] and Miyazaki *et al.* [5] observed the decrease of α_g and α_l with the thickness in addition to the decrease in T_g. It is obvious that the surface effect was not enough to explain both findings simultaneously, hence we have to include an interfacial contribution as well. We did not observe the clear change of α_g or α_l for each layer except for the zero thermal expansivity of the bottom layer, however the decrease in α_g or α_l with the film thickness would be reproduced if the thermal expansivity were given by the average of each layer because the contribution of the bottom

layer becomes dominant as the film thickness decreases. Consider an extreme case in which a thin film consists of the surface and the interfacial layer only, T_g is determined by the surface T_g, resulting in a decrease in T_g, and the thermal expansivity is given by $(d_{\mathrm{suf}}/D)\alpha_{g,\mathrm{suf}}$ or $(d_{\mathrm{suf}}/D)\alpha_{l,\mathrm{suf}}$, resulting in a decrease in the thermal expansivity. Thus, including both the surface and interface effects together, we could understand the decreases of thermal expansivity and T_g with thickness at the same time based on the distributions. It must be emphasized that both the surface and interfacial properties of PS thin films are indispensable for understanding the anomalous film thickness dependences of T_g and α.

We also have to discuss the interdiffusion between *h*-PS and *d*-PS layers to clarify the relation between the molecular mobility and T_g. We focused on the temperature dependence of interfacial roughness between two layers. The ability to evaluate the interfacial roughness is also one of the advantages of the NR measurements. We have prepared the multilayered thin films by the water-floating method, hence it was quite difficult to minimize the interfacial roughness compared to spin-coating or other methods. Even after the preparation of multilayered thin films, the average interfacial roughness ranged from 20 to 30 Å at the interface between different layers. Stamm *et al.* also reported that the interfacial roughness prepared by the water-floating method [17,18] ranged from 10 to 20 Å in spite of careful sample preparation. We wanted to extract the net interfacial broadening due to the interdiffusion as a function of temperature, therefore we defined Δ Roughness by subtracting the roughness at room temperature from the roughness at a given temperature under the assumption that the initial roughness at room temperature was not correlated to the interdiffusion [17,18]. We plotted the temperature dependence of Δ Roughness for the five-layer film in Fig. 8. The Δ Roughness between the fourth and fifth layers was at round 50 Å, and this value was the largest among all of the Δ Roughnesses examined, suggesting that the decrease of T_g enhanced the molecular mobility. Kawaguchi *et al.* [27] also reported a similar enhancement of roughness at the surface region of polymer thin film compared to that of bulk, hence an increase of mobility by a decrease of T_g seems reasonable. Even for the fourth and fifth layer, at which the interface exhibited maximum Δ Roughness, such an increase of roughness due to interdiffusion was about 20% compared to the initial thickness, and the evaluation of thickness worked very well so as not to distinguish each layer independently in the NR measurements. The distribution of thermal expansivity in the multilayered thin films could reproduce that of the total film thickness even above bulk T_g, hence the evaluation of the film thickness and the interfacial roughness above T_g was reliable in spite of the interdiffusion above bulk T_g. As a reference, we also calculated the temperature dependence of root-mean-square displacement (RMSD) of the center of mass of bulk PS. We used the bulk diffusion constant (D) of PS from the works by Karim *et al.* [28] and calculated the temperature dependence of D utilizing the shift factor of PS [28]. Assuming that the interdiffusion is isotropic, we calculated the mean-square displacement (MSD) at a temperature T through a relation $X_{\mathrm{MSD}} = 2D(T)t$, where $D(T)$ and t correspond to the diffusion constant at T and the measurement time, respectively, and we plotted them in Fig. 8 as a solid line. The calculated RMSD almost agreed with the Δ Roughnesses between the second and third layers and between the third and fourth layers, reflecting that the T_g's of the third and fourth layers were almost the same as the bulk T_g. On the other hand, the Δ Roughness between the fourth and fifth layers was the smallest, again suggesting that the increase of T_g suppressed the molecular mobility. We considered that the change of T_g affected the molecular mobility or the temperature dependence of the shift factor of the bulk system. As a result, we observed the correlation between T_g and the molecular mobility.

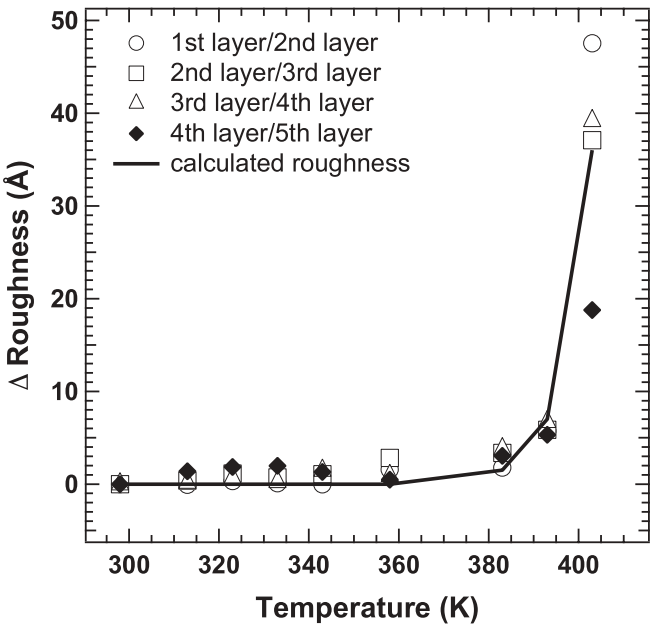

FIG. 8. Temperature dependence of Δ Roughness for the five-layer thin film; solid line correspond to the calculated interdiffusion process based on reptation.

Finally, we should also address the segregation effects because of the weakly unfavorable χ interaction originating from the difference in polarizability between C-H and C-D bonds [29,30]. Experimentally, Bates *et al.* and Green *et al.* evaluated the temperature dependence of the χ parameter of *d*-PS/*h*-PS polymer blend by small-angle neutron scattering (SANS) and elastic recoil detection (ERD) [29–31]. The evaluated χ parameter for our *d*-PS/*h*-PS system was 2.06×10^{-4} at 403 K from their results. This segregation effect [32] was only observed for the following case:

$$\chi < \frac{2}{N},$$

where N is the degree of polymerization. Using an evaluated χ parameter at 403 K, the segregation effect cannot be ignored if N is above 9700. Fortunately, N of our PS was about 7000 and it seems that we can safely ignore the unwanted segregation effect in our multilayered thin films.

IV. CONCLUSION

In this work, we have evaluated the distributions of T_g and α in multilayered thin films consisting of alternatively stacked

d-PS and *h*-PS layers by neutron reflectivity. We explained the reported film thickness dependences of T_g and α based on the distributions, suggesting that T_g of the total film thickness is mainly dominated by the surface T_g while α is determined by the average of each layer. The evaluated roughness was the largest near the surface position and the smallest near the bottom layer among the interfaces examined, showing that the molecular mobility was affected by the change of T_g.

[1] J. A. Forrest and R. A. L. Jones, in *Polymer Surfaces, Interfaces and Thin Film*, edited by A. Karim and S. Kumar (World Scientific, Singapore, 2000), p. 251.

[2] J. A. Forrest, Eur. Phys. J. E **8**, 261 (2002).

[3] J. L. Keddie, R. A. L. Jones, and R. A. Cory, Europhys. Lett. **27**, 59 (1994).

[4] S. Kawana and R. A. L. Jones, Phys. Rev. E **63**, 21501 (2001).

[5] T. Miyazaki, K. Nishida, and T. Kanaya, Phys. Rev. E **69**, 061803 (2004).

[6] T. Kanaya, T. Miyazaki, H. Watanabe, K. Nishida, H. Yamano, S. Tasaki, and D. B. Bucknall, Polymer **44**, 3769 (2003).

[7] G. B. DeMaggio, W. E. Frieze, D. W. Gidley, M. Zhu, H. A. Hristov, and A. F. Yee, Phys. Rev. Lett. **78**, 1524 (1997).

[8] K. Fukao and Y. Miyamoto, Phys. Rev. E **61**, 1743 (2000).

[9] R. Inoue, T. Kanaya, K. Nishida, I. Tsukushi, M. T. F. Telling, B. J. Gabrys, M. Tyagi, C. Soles, and W.-l. Wu, Phys. Rev. E **80**, 031802 (2009).

[10] N. Satomi, A. Takahara, and T. Kajiyama, Macromolecules **32**, 4474 (1999).

[11] C. J. Ellison and J. M. Torkelson, Nat. Mater. **2**, 695 (2003).

[12] R. Inoue, T. Kanaya, K. Nishida, I. Tsukushi, J. Taylor, S. Levett, and B. J. Gabrys, Eur. Phys. J. E **24**, 55 (2007).

[13] P. G. de Gennes, Eur. Phys. J. E **2**, 201 (2000).

[14] J. Gracía-Turiel and B. Jérome, Colloid Polym. Sci. **285**, 1617 (2007).

[15] J. Perlich, V. Korstgens, E. Metwalli, L. Schulz, R. Georgii, and P. Muller-Buchbaum, Macromolecules **42**, 337 (2009).

[16] X. Zhang, K. G. Yager, S. Kang, N. J. Fredin, B. Akgun, S. Styija, J. F. Douglas, A. Karim, and R. L. Jones, Macromolecules **43**, 1117 (2010).

[17] M. Stamm, S. Hüttenbach, G. Reiter, and T. Springer, Europhys. Lett. **14**, 451 (1991).

[18] T. Kuhlmann, J. Kraus, P. Müller-Buschbaum, D. W. Schubert, and M. Stamm, J. Non-Cryst. Solids **235-237**, 457 (1998).

[19] Y. Seo and S. Satija, Langmuir **22**, 7113 (2006).

[20] T. Kanaya, R. Inoue, K. Kawashima, T. Miyazaki, I. Tsukushi, K. Shibata, G. Matsuba, K. Nishida, and M. Hino, J. Phys. Soc. Jpn. **78**, 041004 (2009).

[21] T. Ebisawa, S. Tasaki, Y. Otake, H. Funahashi, K. Soyama, N. Torikai, and Y. Matsushita, Physica B **213**/**214**, 901 (1995).

[22] L. G. Parratt, Phys. Rev. **95**, 359 (1954).

[23] W. E. Wallace, N. C. Beck Tan, and W. L. Wu, J. Chem. Phys. **108**, 3798 (1998).

[24] T. Miyazaki, K. Nishida, and T. Kanaya, Phys. Rev. E **69**, 022801 (2004).

[25] K. Tanaka, Y. Tateishi, Y. Okada, T. Nagamura, M. Doi, and H. Morita, J. Phys. Chem. B **113**, 4571 (2009).

[26] K. S. Gautam, A. D. Schwab, A. Dhinojwala, D. Zhang, S. M. Dougal, and M. S. Yeganeh, Phys. Rev. Lett. **85**, 3854 (2000).

[27] D. Kawaguchi, K. Tanaka, T. Kajiyama, A. Takahara, and S. Tasaki, Macromolecules **36**, 1235 (2003).

[28] A. Karim, A. Mansour, G. P. Felcher, and T. P. Russell, Phys. Rev. B **42**, 6846 (1990).

[29] F. S. Bates and G. D. Wignall, Macromolecules **19**, 934 (1986).

[30] F. S. Bates and G. D. Wignall, Phys. Rev. Lett. **57**, 1429 (1986).

[31] P. F. Green and B. L. Doyle, Macromolecules **20**, 2471 (1987).

[32] *Polymers and Surfaces: A Versatile Combination*, edited by H. Hommel (Research Signpost, 1998).